Energy-Based Trajectory Tracking Control of Under-actuated Unmanned Surface Vessels

Weijun Zhou, Zishi Xu, Yongxin Wu, Xiang Ji, Yanjun Li

Energy-Based Trajectory Tracking Control of Under-actuated Unmanned Surface Vessels

Weijun Zhou[a], Zishi Xu[b], Yongxin Wu[c], Ji Xiang[b], Yanjun Li[a,*]

[a]School of Information and Electrical Engineering, Hangzhou City University, Hangzhou, 310015, P. R. China (e-mails: {zhouwj;liyanjun}@hzcu.edu.cn).
[b]Zhejiang University, Hangzhou, 310015, P. R. China (e-mails: {xuzishi;jxiang}@zju.edu.cn).
[c]Université de Franche-Comté, SUPMICROTECH, CNRS, Institut FEMTO-ST, 25000 Besançon, France (e-mail: yongxin.wu@femto-st.fr)

Abstract

In this paper, a novel energy-based trajectory tracking control strategy for under-actuated unmanned surface vessels (USVs) in the presence of unknown environmental disturbances is presented. The port-Hamiltonian framework is utilized to propose a passivity-based control model in body-fixed coordinates of the USVs. An adaptive disturbance estimation method is detailed and used to accurately estimate the environmental disturbances affecting USV motion. Furthermore, a passive and Hamiltonian structure-preserving controller is employed to achieve the desired trajectory of the USV system, and the stability of the desired target dynamic system is rigorously proven. The effectiveness of the proposed controller is demonstrated through simulations and experiments on a USV experimental platform, showcasing its capability of trajectory tracking performance and mitigating the effects of disturbances.

Keywords: Energy based control; Port-Hamiltonian system; Trajectory tracking control; Under-actuated USV

1. Introduction

In recent decades, differential-driven unmanned surface vessels (USVs) have gained increasing popularity in military and civilian applications due to their operational convenience and simple mechanical structure. These types of USVs are typically considered under-actuated due to their mechanical configuration. Differential-driven USVs typically feature only two propellers installed in parallel on both sides of the vessel, with each propeller providing independent thrust to enable the vessel's motion. Specifically, the surge translational motion is obtained by calculating the sum of the thrust of the two propellers, while the yaw rotational motion is achieved by calculating the difference between the thrust of the two propellers. However, the force in the sway direction cannot be provided, resulting in under-actuation in differential-driven USVs.

Compared to fully actuated and over-actuated vehicles, the tracking control problem of underactuated USVs presents a significant challenge in the field of marine robotics. Differential-driven USVs, in particular, face difficulties in accurately tracking desired trajectories due to their limited control inputs in relation to their degrees of freedom. Most under-actuated systems are not fully feedback linearizable and exhibit nonholonomic constraints, which further complicates the control design process. Many studies have been dedicated to the tracking control of under actuated USVs. The Line-of-Sight(LOS)-based path following control approach [1] for under-actuated unmanned vessels includes orienting the vessel toward the desired path, following the path along straight line segments, and adjusting the vessel's orientation near each waypoint based on the next waypoint to form a smooth curve. Thus, the control problem, which initially has 3 DoFs (position, orientation, and speed), is reduced to a 2-DoF problem involving only orientation and speed. A linear time-varying control approach [2] that utilizes a cascaded control strategy is presented, and this method is used to design a controller for an under-actuated ship. The proposed method employs a second-order integrator system, forming a cascaded control structure to achieve the desired tracking performance. The back-stepping control approach is also commonly employed to address the control challenges posed by under-actuated USVs [3][4][5][6]. In [7], an adaptive switching supervisory control strategy that uses the backstepping technique is integrated with a non-linear Lyapunov-based tracking control law to drive the position tracking error of a system toward a neighborhood of the origin, which can be arbitrarily small. In [8], the authors investigated the tracking control problem of a surface vessel following a desired trajectory generated by a reference model vessel. The approach employed in this study is the dynamic surface method, which is an approximate back-stepping technique introduced to address the challenges of differentiating virtual controls in the traditional back-stepping method. In [9], sliding mode control is utilized to transform the trajectory tracking problem into a velocity tracking problem. Two sliding surfaces are employed to decouple the problem, with one surface controlling the forward velocity and the other surface controlling the lateral velocity. In addition to the mentioned technique, other control methods, such as proportional-integral-differential (PID) control [10] and the Lyapunov direct method [7], have also been applied in the trajectory tracking

☆This research was supported in part by Zhejiang Provincial Natural Science fund(LQ21F030008); in part by the French EIPHI Graduate School(ANR-17-EURE-0002); in part by the French ANR IMPACTS Project(ANR-21-CE48-0018)

*Corresponding author
Email address: liyanjun@hzcu.edu.cn (Yanjun Li)

control of underwater USVs.

The port-Hamiltonian system (PHS) formulation [11] and passivity-based control [12] have been widely used and demonstrated to be effective for the modeling, analysis and control of non-linear mechanical systems. The port-Hamiltonian framework offers a systematic approach for interpreting control actions in terms of energy conservation and dissipation principles, providing a clear physical interpretation of the control strategies used in a system. Energy-based control, such as the interconnection and damping assignment passivity-based control(IDA-PBC)[12][13], is employed for the optimization of energy control. USVs are considered as efficient energy conversion devices, capable of transforming input energy into output energy effectively. The primary objective of employing the IDA-PBC method is to optimize the input and output energy of the entire system, with the ultimate goal of minimizing energy consumption. Many studies have been dedicated to the IDA-PBC control of physical systems [14][15][16][17][18]. The principal is to utilize the principles of dissipation and energy shaping (ES) to reconfigure the open-loop system into the desired dynamic system while also preserving the port-Hamiltonian structure. The control problem of USVs in the port-Hamiltonian framework [19][20] has gained much attention in recent years. In [20], a comprehensive survey on the motion control problem of marine vehicles is provided , focusing on the application of the energy shaping principle. A hybrid control law based on backstepping and a passivity-based control technique is proposed for the speed tracking of under-actuated USVs using the LOS method [21]. The authors presented an observer-based state-error port-Hamiltonian controller with a nonlinear disturbance observer for the trajectory tracking problem in [22]. An IDA-PBC controller with integral action was designed for fully actuated marine vehicles in [23]. A family of trajectory tracking controllers for a fully actuated marine craft in the port-Hamiltonian (pH) framework using virtual differential passivity-based control (v-dPBC) was proposed in [24].

The primary contribution of this paper is the development of an energy-based trajectory tracking control strategy for under-actuated USVs operating in the presence of unknown environmental disturbances. A reduced PHS model in body-fixed coordinates is proposed to accurately capture the system's physical characteristics for control purposes. By designing an adaptive estimator, the disturbance is continuously updated and refined, enhancing the accuracy of the overall control system. Moreover, the control strategy employs the IDA-PBC method, accounting for the under-actuated nature of the system. Notably, other approaches mentioned earlier are applicable in fully actuated scenarios. We have

By using the port-Hamiltonian structure, we show that the closed loop system is asymptotically stable. Furthermore, the effectiveness of the proposed method is demonstrated through simulation and experimental implementation, resulting in the successful tracking of desired trajectories by the unmanned surface vessel.

In Section 2, a concise summary of the existing results on port-Hamiltonian systems and the IDA-PBC control method is provided. In Section 3, a summary on the body-fixed coordinates model of the differential-driven USV in the PH framework is provided. In Section 4, the derivation of an adaptive disturbance estimation method and the development of energy-based control laws are presented. Additionally, the closed-loop stability analysis is presented in the same section. In Section 5, simulations and the experimental setup are utilized to validate the proposed model and control law. The paper ends with some conclusions and perspectives in Section 6.

2. Preliminaries

Port-Hamiltonian systems excel in modeling multi-physical systems, where different physical domains interact. An electrically driven USV is a common example of a system that converts electrical energy into mechanical energy for motion. Understanding these energy transformations is crucial to grasp the system's behavior. This physical insight provides a clear interpretation of control behaviors , as controllers designed using passivity-based control account for the energy exchanges, including interactions between different physical domains, and between the system and its environment. Furthermore, through stability and robustness analysis of passive systems, the improved robustness and stability enhance the effectiveness of closed-loop systems that employ energy-based control strategies. This paragraph explaining the rationale and necessity of utilizing Port-Hamiltonian Systems (PHS) has been incorporated into the article.This physical insight provides a clear interpretation of control behaviors , as controllers designed using passivity-based control account for the energy exchanges, including interactions between different physical domains, and between the system and its environment. Furthermore, through stability and robustness analysis of passive systems, the improved robustness and stability enhance the effectiveness of closed-loop systems that employ energy-based control strategies.

In this section, a brief overview of the literature on port-Hamiltonian systems and the IDA-PBC control methodology is provided.

2.1. Port-Hamiltonian system

The port-Hamiltonian systems [25] are described as follows:

$$\begin{cases} \dot{x} = [J(x) - R(x)]\frac{\partial H}{\partial x}(x) + g(x)u \\ y = g^T(x)\frac{\partial H}{\partial x}(x) \end{cases} \tag{1}$$

where $x \in \mathbb{R}^n$ represents the system's state, the input variable $u \in \mathbb{R}^m$ represents the control input, and the output variable $y \in \mathbb{R}^m$ represents the system's output. The Hamiltonian function $H(x,t) \in \mathbb{R}$ captures the system's energy, while the matrices $J \in \mathbb{R}^{n\times n}$ and $R \in \mathbb{R}^{n\times n}$ are skew-symmetric and symmetric semi-positive definite matrices, respectively. These matrices arise from the expansion of Hamilton's canonical equations and are commonly used to describe fully actuated mechanical systems [11], including systems subject to certain nonholonomic constraints.

2.2. IDA-PBC method

The main idea of IDA-PBC [12][13] is to match the dynamics of the open-loop system with a desired target system using state feedback control, as depicted in figure 1. The control law enforces the desired storage function H_d on the closed-loop system, thereby ensuring its passivity and subsequent stability. We briefly review the fundamental principles of the IDA-PBC method. The approach is applied to an open-loop port-Hamiltonian system described by Equation (1), with the objective of stabilizing it around a desired equilibrium point x^*.

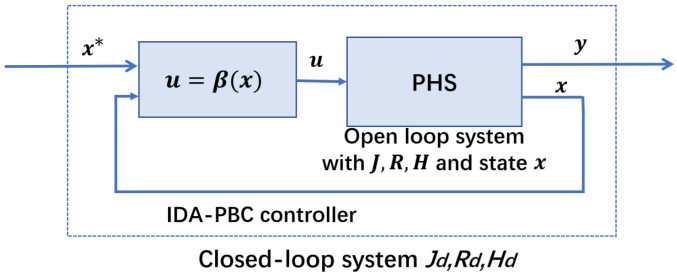

Figure 1: Control design of closed loop system

The asymptotically stable PHS target system is defined as :

$$\dot{x} = (J_d - R_d)\frac{\partial H_d}{\partial x} \tag{2}$$

with matrices $J_d(x) = -J_d(x)^T$ and $R_d(x) = R_d(x)^T \leq 0$, and the desired Hamiltonian function H_d verifies the PDE:

$$g^{\perp}(J_d - R_d)\frac{\partial H_d}{\partial x} = g^{\perp}(J - R)\frac{\partial H}{\partial x} \tag{3}$$

where $g^{\perp}$ is a full rank left annihilator of g, i.e.,$g^{\perp}g = 0$. The PDE is a so-called matching condition. Additionally, the Hamiltonian function $H_d(x)$ needs to satisfy the following requirements:

$$x^* = \text{argmin} H_d(x). \tag{4}$$

The closed-loop port-controlled Hamiltonian system is governed by the feedback law as follows:

$$u = \beta(x) = (g^T g)^{-1} g^T ((J_d - R_d)\frac{\partial H_d}{\partial x} - (J - R)\frac{\partial H}{\partial x}) \tag{5}$$

Moreover, this system exhibits local asymptotic stability at the equilibrium point x^*. [12] can be referenced for comprehensive explanations and proofs.

3. Problem statement

3.1. Mathematical model and dynamics of USV in PH form

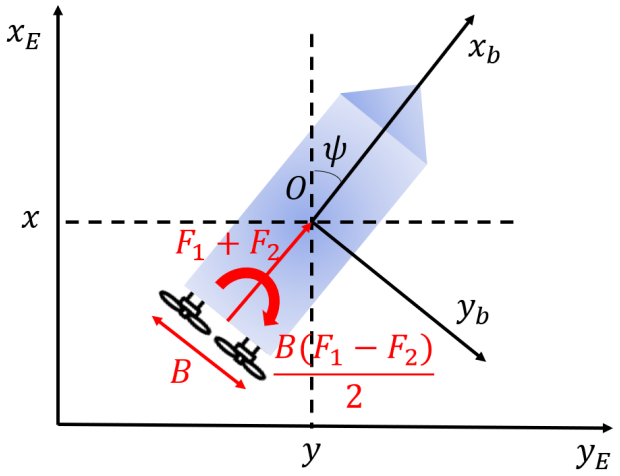

Figure 2: Coordinate system in 2D describing the motion of a differential-driven USV

In marine craft modeling for guidance, navigation, and control, the body frame is commonly employed as a moving coordinate frame that is fixed to the vessel, with its origin at the center of gravity O. The body frame provides a concise and convenient representation of the craft's motion and dynamics with respect to its own orientation and position. As shown in Figure (2), the axes x_b, y_b, and z_b point to the surge, sway direction, and upward direction of the vessel, respectively. The world frame is fixed to an inertial reference frame and provides an absolute reference for the craft's motion and dynamics. In the context of marine craft motion, the world frame typically has one axis pointing vertically downward and the other two axes aligned with the geographic coordinate system. The axes x_E, y_E, and z_E point to the north, east, and vertically downward, respectively, with E being the origin of the world frame.

The mathematical model of a USV [26],[27] typically represents a rigid body subject to external torques and forces with its coordinate depicted in Figure 2:

$$\begin{cases} \dot{q} = J(q)v, \\ M\dot{v} = -C(v) - D(v)v + \tau_c + \tau_d \end{cases} \tag{6}$$

where $q = \begin{bmatrix} x & y & \psi \end{bmatrix}^T$ is the displacement vector in the earth frame. x and y represent the positions along x_E and y_E in the earth frame, respectively, while ψ denotes the heading orientation of the USV. $v = \begin{bmatrix} u & v & r \end{bmatrix}^T$ denote the velocity vector in the body frame. u, v, and r are the linear velocity in the surge and sway directions and the angular velocity, respectively. $M = \text{diag}(m_{11}, m_{22}, m_{33})$ is the inertia matrix accounting for added mass, $\tau_c \in \mathbb{R}^3$ is the vector for controlling forces and moments, and $\tau_d \in \mathbb{R}^3$ is the disturbance. $J(q) \in \mathbb{R}^{3\times3}$ is the rotation matrix:

$$J(q) = \begin{bmatrix} R(\psi) & 0_{2\times1} \\ 0_{1\times2} & 1 \end{bmatrix}, R(\psi) = \begin{bmatrix} \cos(\psi) & -\sin(\psi) \\ \sin(\psi) & \cos(\psi) \end{bmatrix} \quad (7)$$

The Coriolis and centripetal matrix denoted as $C(v)$ represents the effects of the Coriolis force and centripetal force. The damping matrix denoted as $D(v)$ captures the damping effects in the USV's motion:

$$C(v) = \begin{bmatrix} 0 & 0 & -m_{22}v \\ 0 & 0 & m_{11}u \\ m_{22}v & -m_{11}u & 0 \end{bmatrix}, D(v) = \begin{bmatrix} d_{11} & 0 & 0 \\ 0 & d_{22} & 0 \\ 0 & 0 & d_{33} \end{bmatrix} \quad (8)$$

The propulsion system of a USV consists of two electric-powered motors that drive two propellers symmetrically installed at the stern of the vessel, as depicted in Figure 2. The control of the two motors in a USV can be decomposed into torque control in the surge direction and torque control in the rotation direction:

$$\tau_c = \begin{bmatrix} \tau_u \\ \tau_v \\ \tau_r \end{bmatrix} = \begin{bmatrix} F_1 + F_2 \\ 0 \\ \frac{B(F_1 - F_2)}{2} \end{bmatrix} \quad (9)$$

where F_1 and F_2 represent the propulsive forces generated by the permanent magnet synchronous motors driving the propellers. B denotes the distance between the propellers.

According to the research of [23], the port-Hamiltonian System (PHS) form for a full-actuated USV can be expressed as follows:

$$\begin{bmatrix} \dot{q} \\ \dot{p} \end{bmatrix} = \begin{bmatrix} 0 & J(q) \\ -J^T(q) & -J_2(p) \end{bmatrix} \begin{bmatrix} \frac{dH}{dq} \\ \frac{dH}{dp} \end{bmatrix} + \begin{bmatrix} 0_{3\times3} \\ I_3 \end{bmatrix} (\tau_c + \tau_d) \quad (10)$$

with $p = M \begin{bmatrix} u & v & r \end{bmatrix}^T$ and $J_2(p) = C(v) + D(v)|_{v=M^{-1}p}$, $J_2(p) + J_2^T(p) > 0$

The Hamiltonian for the system is defined as $H(p,q) = \frac{1}{2} p^T M^{-1} p + V(q)$, where p denotes the generalized momenta, q denotes the generalized coordinates, M denotes the inertia matrix, and $V(q)$ represents the potential energy caused by gravitational forces. The first term, $\frac{1}{2} p^T M^{-1} p$, corresponds to the system's kinetic energy and characterizes its motion properties. The second term, $V(q)$, captures the potential energy associated with the gravitational forces acting on the system.

3.2. PHS in body fixed frame

We propose a novel PH formulation for under-actuated USVs for trajectory tracking control. First, the kinematic variables x and y are transformed from the world frame into the body frame.

In the conventional modeling approach, the tracking error of the vessel's trajectory (x, y, ψ) and the desired trajectory (x_d, y_d, ψ_d) coordinates of the USV are typically computed with respect to the world frame. To simplify the control process, that is, to effectively control the surge and sway motion of the USV, these trajectories are then transformed into the body-fixed frame using transformation matrices $R(\psi)$. It is feasible to express the surge displacement, denoted as s, and the sway displacement, denoted as t, in terms of the x_b and y_b coordinates in the body-fixed frame of the USV. This relationship between the surge and sway displacements and the x and y coordinates can be expressed mathematically as follows:

$$\eta_r = \begin{bmatrix} s \\ t \end{bmatrix} = R(\psi)^T \begin{bmatrix} x \\ y \end{bmatrix} \quad (11)$$

where η_r denote the translation displacement matrix.

By deriving Equation (11), the time derivatives of the surge and sway displacements, denoted as $\dot{s}$ and $\dot{t}$, respectively, can be expressed in terms of the linear and angular velocities of the USV as follows:

$$\dot{\eta} = \begin{bmatrix} \dot{s} \\ \dot{t} \\ \dot{\psi} \end{bmatrix} = J_\eta(\eta) \begin{bmatrix} u \\ v \\ r \end{bmatrix} \quad (12)$$

with $J_\eta(\eta) = \begin{bmatrix} 1 & 0 & t \\ 0 & 1 & -s \\ 0 & 0 & 1 \end{bmatrix}$

The original PH form of the USV then becomes:

$$\begin{bmatrix} \dot{\eta} \\ \dot{p} \end{bmatrix} = \begin{bmatrix} 0 & J_\eta(\eta) \\ -J_\eta^T(\eta) & -J_2(p) \end{bmatrix} \begin{bmatrix} \frac{dH}{d\eta} \\ \frac{dH}{dp} \end{bmatrix} + \begin{bmatrix} 0_{3\times3} \\ I_3 \end{bmatrix} (\tau_c + \tau_d) \quad (13)$$

Remark 1. *The proposed model is based on the Port-Hamiltonian framework, which preserves the physical and nonlinear characteristics of the system. This enables us to employ under-actuated IDA-PBC control design methods. Furthermore, by transforming the position error from the world coordinate system to the body coordinate system, the generation of velocity commands becomes more intuitive and aligned with the ship's motion in its local frame of reference as the two are now all defined with respect to the body coordinate system.*

4. Control design for under-actuated USV

The goal is to stabilize the under-actuated USV to track differentiable reference trajectories η_{rd} by regulating τ_c. η_{rd} is defined as follows:

$$\eta_{rd} = \begin{bmatrix} s_d & t_d \end{bmatrix}^T = R(\psi)^T \begin{bmatrix} x_d \\ y_d \end{bmatrix} \quad (14)$$

where s_d, r_d, x_d, and y_d are the desired surge, sway displacement and desired position along x_E and y_E in the earth frame, respectively.

A control law of the USV system (13) using an IDA-PBC design is proposed to ensure that:

$$\lim_{t\to+\infty} \eta_r(t) = \eta_{rd}(t) \quad (15)$$

The closed-loop control schema is shown in Figure 3. The tracking control problem of under-actuated unmanned surface vessels is challenging due to the lack of control input in the sway direction.

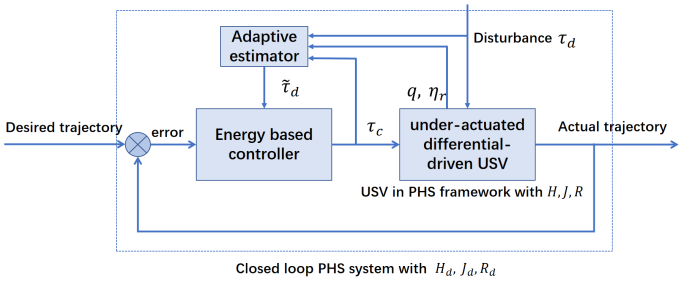

Figure 3: Detailed control scheme of USV using Adaptive estimator + Error IDA-PBC control

4.1. Adaptive estimator of the disturbances

The unknown disturbances are estimated from the open loop dynamics using the immersion and invariance method [28], as outlined in the following proposition.

Proposition 2. *Considering the USV system* (13)*, the estimation $\tilde{\tau}_d$ converges to the real disturbance asymptotically with the following adaptive estimation law:*

$$\tilde{\tau}_d = -\alpha p + \alpha \int (-J_\eta^T \frac{\partial H}{\partial \eta} - J_2 \frac{\partial H}{\partial p} + \tau_c - \tilde{\tau}_d)dt \tag{16}$$

with the tuning parameter $\alpha > 0$.

Proof. We define the vector of the estimation errors z_τ, in which the functions $\hat{\tau}_d$ and $\beta(p)$ are the state-independent part and the state-dependent part of the estimator $\tilde{\tau}_d$, as follows:

$$z_\tau = \tilde{\tau}_d - \tau_d = \beta(p) + \hat{\tau}_d - \tau_d \tag{17}$$

Computing the time derivative of (17) and substituting the system dynamic yields :

$$\dot{z}_\tau = \dot{\hat{\tau}}_d - \nabla_p \beta(-J_\eta^T \frac{\partial H}{\partial \eta} - J_2 \frac{\partial H}{\partial p} + \tau_c + (-z_\tau + \tilde{\tau}_d + \beta)) - \dot{\tau}_d \tag{18}$$

We define $\dot{\hat{\tau}}_d = -\alpha(-J_{\eta_r}^T \frac{\partial H}{\partial \eta_r} - J_2 \frac{\partial H}{\partial p} + \tau_c + (\tilde{\tau}_d + \beta))$ and $\beta = -\alpha p$, which correspond to the adaptation law (16). The derivative of z_τ gives domain of attractions

$$\dot{z}_\tau = -\alpha z_\tau - \dot{\tau}_d \tag{19}$$

The Lyapunov candidate function of the disturbance observer is defined as follows:

$$V_e = \frac{1}{2} z_\tau^T z_\tau \tag{20}$$

The time derivative of the Lyapunov candidate function becomes:

$$\dot{V}_e = z_\tau^T \dot{z}_\tau = z_\tau^T(-\alpha z_\tau - \dot{\tau}_d) = -\alpha z_\tau^T z_\tau - z_\tau^T \dot{\tau}_d \tag{21}$$

We have the following inequality:

$$\begin{aligned} 4\epsilon^2 z_\tau^T z_\tau + 4\epsilon z_\tau^T \dot{\tau}_d + \dot{\tau}_d^T \dot{\tau}_d = (2\epsilon z_\tau + \dot{\tau}_d)^2 \geq 0 \\ \Rightarrow -z_\tau^T \dot{\tau}_d \leq \epsilon z_\tau^T z_\tau + \frac{1}{4\epsilon} \dot{\tau}_d^T \dot{\tau}_d \end{aligned} \tag{22}$$

where ϵ is a small positive constant. We have then:

$$\dot{V}_e \leq -\lambda_{min}(\alpha) z_\tau^T z_\tau + \epsilon z_\tau^T z_\tau + \frac{1}{4\epsilon} \dot{\tau}_d^T \dot{\tau}_d \tag{23}$$

We assume that $\|\dot{\tau}_d\| \leq \xi$; thus, the following can be obtained:

$$\dot{V}_e \leq -2(\lambda_{min}(\alpha) - \epsilon) V_e + \frac{\xi^2}{4\epsilon} \leq -K_0 V_e + c \tag{24}$$

with $K_0 = 2(\lambda_{min}(\alpha) - \epsilon)$, $c = \frac{\xi^2}{4\epsilon}$ and $\lambda_{min}(\alpha)$ is the smallest eigenvalue of α.

To ensure that $K_0 > 0$, we select the matrix $K_0 = \text{diag}(k_{10}, k_{20}, k_{30})$ and parameter ϵ.

By solving the inequality (24), the condition $\dot{V}_e \leq 0$ can be verified when:

$$0 \leq V_e \leq \frac{c}{K_0} + (V(0) - \frac{c}{K_0}) e^{-K_0 t} \tag{25}$$

Moreover, the disturbance estimation error converges to a neighborhood Ω_b of the origin with the radius $R_d = \frac{\xi}{2\sqrt{\epsilon(\lambda_{min}(\alpha) - \epsilon)}}$. □

4.2. Energy-based Robust tracking control of under-actuated USV

We define the tracking errors in the body-fixed frame as

$$\tilde{\eta}_r = \eta_r - \eta_{rd} \tag{26}$$

Given Equation (9), the control variable torque in the y_b direction τ_v is null , which render control in this direction unattainable because of the mechanical structure of the propeller. To overcome this problem, we consider a fixed point on the vessel body. This approach mitigates the matrix singularity issues that may arise in subsequent controller calculations due to underactuation. Further details regarding the redefinition of state variables are provided in the Appendix.

By considering a position error δ with respect to the center of mass in the surge direction, we define $\Delta = \begin{bmatrix} \delta & 0 \end{bmatrix}^T$, and the new tracking error is then:

$$\zeta = \tilde{\eta}_r - \Delta \tag{27}$$

The objective is to design an energy-based controller so that the closed-loop dynamics have the following desired tracking error dynamic in the port-Hamiltonian form:

$$\begin{bmatrix} \dot{\zeta} \\ \dot{\tilde{p}} \end{bmatrix} = \begin{bmatrix} S_{11} & S_{12} \\ -S_{12}^T & S_{22} \end{bmatrix} \nabla H_d \tag{28}$$

where $\tilde{p} = p - p_d = \begin{bmatrix} u - u_d & v - v_d & r - r_d \end{bmatrix}^T$ with $p_d = \begin{bmatrix} u_d & v_d & r_d \end{bmatrix}^T$ denotes the desired generalized momenta and

the tracking error of the generalized momenta, with u_d,v_d and r_d being the desired linear velocity in the surge and sway directions and the desired angular velocity, respectively. S_{11} a 2×2 matrix, S_{12} a 2×3 matrix and S_{22} a 3×3 are functions to be selected. S_{11} and S_{22} are strictly negative.

The desired Hamiltonian function H_d is defined as follows:

$$H_d = \frac{1}{2}\tilde{p}^T M^{-1}\tilde{p} + V_d(\zeta) \tag{29}$$

The first term represents the kinetic energy, while the second is the desired potential energy considering the added distance :

$$V_d = \zeta^T K_d \zeta \tag{30}$$

with $K_d = \begin{bmatrix} K_{d_1} & 0 \\ 0 & K_{d_2} \end{bmatrix}$, K_{d_1} and K_{d_2} are positive defined.

The gradient of the Hamiltonian function and the desired energy function is then defined as

$$\nabla H_d = \begin{bmatrix} \frac{\partial H_d}{\partial \zeta} \\ \frac{\partial H_d}{\partial \tilde{p}} \end{bmatrix} = \begin{bmatrix} \nabla V_d \\ M^{-1}\tilde{p} \end{bmatrix}. \tag{31}$$

$$\nabla V_d = 2K_d\zeta \tag{32}$$

We design the control law as follows. First, we write the dynamic of the position error by substituting the time derivative of $\tilde{\eta}_r$ by the state equation (10) and the desired state equation:

In this case, we calculate $\dot{\zeta}$:

$$\begin{aligned}
\dot{\zeta} =& \frac{d}{dt}(\tilde{\eta}_r - \Delta) = -S_r(R^T\tilde{\eta}_r - \begin{bmatrix}\delta \\ 0\end{bmatrix}) - S_r\Delta + \begin{bmatrix}u \\ v\end{bmatrix} - R^T\begin{bmatrix}\dot{x}_d \\ \dot{y}_d\end{bmatrix} \\
=& -S_r(R^T\tilde{\eta}_r - \begin{bmatrix}\delta \\ 0\end{bmatrix}) + \underbrace{\begin{bmatrix}1 & 0 \\ 0 & -\delta\end{bmatrix}}_{P}\begin{bmatrix}u_d \\ r_d\end{bmatrix} + \begin{bmatrix}1 & 0 \\ 0 & -\delta\end{bmatrix}\begin{bmatrix}\tilde{u} \\ \tilde{r}\end{bmatrix} + \begin{bmatrix}0 \\ v\end{bmatrix} \\
& - R^T\begin{bmatrix}\dot{x}_d \\ \dot{y}_d\end{bmatrix} \\
\equiv& S_{11}\nabla V_d + S_{12}M^{-1}\tilde{p}
\end{aligned} \tag{33}$$

with $S_r = \begin{bmatrix}0 & -r \\ r & 0\end{bmatrix}$

We define $S_{12} = \begin{bmatrix}1 & 0 & 0 \\ 0 & 0 & -\delta\end{bmatrix}$ to eliminate $M^{-1}\tilde{p}$, while $S_{11} = \begin{bmatrix}-1 & \frac{r}{2K_{d_2}} \\ -\frac{r}{2K_{d_1}} & -1\end{bmatrix}$ to eliminate the algebraic ring term of $S_r(R^T\tilde{\eta}_r - \begin{bmatrix}\delta \\ 0\end{bmatrix})$, with S_{11} negatively defined.

$$\begin{bmatrix}u_d \\ r_d\end{bmatrix} = P^{-1}(-2K_d(\tilde{\eta}_r - \Delta) - \begin{bmatrix}0 \\ v\end{bmatrix} + R^T\begin{bmatrix}\dot{x}_d \\ \dot{y}_d\end{bmatrix}) \tag{34}$$

with $v_{rd} = \begin{bmatrix}u_d \\ r_d\end{bmatrix} = WM^{-1}p_d$.

In the second step of the design, we need to ensure that the dynamics of $\tilde{p}$ are as desired by using V_d as the energy equation.

We then compute the time derivative of $\tilde{p}$:

$$\begin{aligned}
\dot{\tilde{p}} &= \dot{p} - \dot{p}_d && (35)\\
&= -J_\eta(\eta)^T\nabla V - J_2(p)M^{-1}p + \tau_c \\
&\quad + \tilde{\tau}_d - \dot{p}_d \\
&\equiv -S_{12}^T\nabla V_d + S_{22}M^{-1}\tilde{p} && (36)
\end{aligned}$$

Due to the under-actuated nature of the system, the control variable in the sway direction $\tau_v = 0$. We multiply Equation (35) by W. Then, by isolating $\begin{bmatrix}\tau_u & \tau_v & \tau_r\end{bmatrix}^T$ from (35), we derive the control law that asymptotically tracks the trajectory η_{rd}:

$$\begin{aligned}
\begin{bmatrix}\tau_u \\ \tau_r\end{bmatrix} =& W(J_2(p)M^{-1}p - S_{12}^T\nabla V_d + S_{22}M^{-1}\tilde{p} - \tilde{\tau}_d) + W\dot{p}_d \\
=& W(J_2(p)M^{-1}p - S_{12}^T\nabla V_d + 2K_dS_{12}\Delta + S_{22}M^{-1}\tilde{p} \\
& - \tilde{\tau}_d) + WMW^{-1}\begin{bmatrix}\dot{u}_d \\ \dot{r}_d\end{bmatrix}
\end{aligned} \tag{37}$$

4.3. Stability analysis

Proposition 3. *We consider the under-actuated USV dynamics* (13) *with the following control law:*

$$\begin{aligned}
\begin{bmatrix}\tau_u \\ \tau_r\end{bmatrix} =& W(J_2(p)M^{-1}p - S_{12}^T\nabla V_d + S_{22}M^{-1}\tilde{p} - \tilde{\tau}_d) + W\dot{p}_d \\
=& W(J_2(p)M^{-1}p - S_{12}^T\nabla V_d + 2K_dS_{12}\Delta + S_{22}M^{-1}\tilde{p} \\
& - \tilde{\tau}_d) + WMW^{-1}\begin{bmatrix}\dot{u}_d \\ \dot{r}_d\end{bmatrix} \\
\textit{with} \quad W =& \begin{bmatrix}1 & 0 & 0 \\ 0 & 0 & 1\end{bmatrix}
\end{aligned} \tag{38}$$

The closed loop system is asymptotically stable with respect to the disturbance τ_d.

Proof. The asymptotic stability of the under-actuated USV position vector η_r to the time-varying reference η_{rd} is established by proving the asymptotically stability of the equilibrium. This is achieved by studying the derivative of the error system Hamiltonian function H_d by considering it as a Lyapunov candidate function.

First, we analyze the equilibrium point of the closed-loop error system (28), which is determined by:

$$\begin{bmatrix}\dot{\zeta} \\ \dot{\tilde{p}}\end{bmatrix} = \begin{bmatrix}S_{11} & S_{12} \\ -S_{12}^T & S_{22}\end{bmatrix}\begin{bmatrix}2K_d\zeta \\ M^{-1}\tilde{p}\end{bmatrix} = 0 \tag{39}$$

From Equation (39), it is straightforward to determinate that the only equilibrium of the closed-loop error system is $\begin{bmatrix}\zeta & \tilde{p}\end{bmatrix}^T = \begin{bmatrix}0 & 0\end{bmatrix}^T$.

We recall the desired Hamiltonian function by substituting V_d by equation (30) and demonstrate its positivity :

$$H_d = \frac{1}{2}\tilde{p}^T M^{-1}\tilde{p} + \zeta^T K_d\zeta \tag{40}$$

The matrix M is positive by definition. Consequently, the first term associated with kinetic energy, represented by the quadratic form $\frac{1}{2}\tilde{p}^T M^{-1}\tilde{p}$, also maintains a positive value.

Let us examine the second term within the desired Hamiltonian function. The desired potential energy, denoted as $V_d = \zeta^T K_d \zeta$, where K_d is positively defined. The quadratic form V_d is consequently also positively defined.

The desired Hamiltonian function of closed-loop system $H_d = \frac{1}{2}\tilde{p}^T M^{-1}\tilde{p} + \zeta^T K_d \zeta$ is minimum when $\tilde{p} = 0_{3\times1}$ and $\zeta = 0_{2\times1}$.

We compute the derivative of H_d with respect to time along the trajectories of the dynamics as follows:

$$\begin{aligned}
\dot{H}_d &= \begin{bmatrix}(\frac{\partial H_d}{\partial \zeta})^T & (\frac{\partial H_d}{\partial \tilde{p}})^T\end{bmatrix}\begin{bmatrix}\dot{\zeta}\\ \dot{\tilde{p}}\end{bmatrix} \\
&= (\frac{\partial H_d}{\partial \zeta})^T(S_{11}\nabla V_d + S_{12}M^{-1}\tilde{p}) \\
&\quad +(\frac{\partial H_d}{\partial \tilde{p}})^T(-S_{12}^T\nabla V_d + S_{22}M^{-1}\tilde{p}) \\
&= (\frac{\partial H_d}{\partial \zeta})^T S_{11}\frac{\partial H_d}{\partial \zeta} + (\frac{\partial H_d}{\partial \zeta})^T S_{12}\frac{\partial H_d}{\partial \tilde{p}} \\
&\quad +(\frac{\partial H_d}{\partial \tilde{p}})^T(-S_{12}^T)\frac{\partial H_d}{\partial \zeta} + (\frac{\partial H_d}{\partial \tilde{p}})^T S_{22}\frac{\partial H_d}{\partial \tilde{p}} \\
&= (\frac{\partial H_d}{\partial \zeta})^T S_{11}\frac{\partial H_d}{\partial \zeta} + (\frac{\partial H_d}{\partial \tilde{p}})^T S_{22}\frac{\partial H_d}{\partial \tilde{p}} \\
&= 4\zeta^T K_d S_{11} K_d \zeta + \tilde{p}^T M^{-1} S_{22} M^{-1}\tilde{p} \qquad (41)
\end{aligned}$$

Given that matrices S_{11} and S_{22} are negatively defined, the two quadratic terms in Equation (41) are strictly negative. Consequently, $\dot{H}_d$ is strictly negative.

To simplify the demonstration, we consider $z = \begin{bmatrix}\zeta & \tilde{p}\end{bmatrix}^T$. From the preceding proof, we can conclude that for the unique equilibrium $z = 0_{5\times1}$:

$$\begin{cases} \dot{H}_d < 0 \ , \forall z \neq 0_{5\times1} \\ \dot{H}_d = 0 \ , z = 0_{5\times1} \end{cases} \qquad (42)$$

Thus H_d is a Lyapunov function candidate for the closed loop system. Using the positivity of H_d we can write:

$$\begin{cases} \lim_{t\to\infty} H_d(z) = 0 \\ \lim_{t\to\infty} z = 0_{5\times1} \end{cases} \qquad (43)$$

We conclude that the closed loop system of under-actuated USV using the non linear state feedback (38) is globally asymptotically stable. By definition, the domain of attraction of the controller is $z \in \mathbb{R}^5$, indicating that for all physically attainable state variables, the closed-loop system demonstrates asymptotic stability.

□

Proposition 4. *Consider the USV system described by Equation (6) in the presence of external disturbances. When the robust controller specified in Equation (38), incorporating the estimator (16), is employed for the closed-loop system, the entire system's stability is guaranteed to be uniformly ultimately bounded (UUB) by appropriately tuning selected parameters.*

Proof. The stability of the entire system, taking external disturbances into account, is determined by the Lyapunov candidate function as follows:

$$V = H_d + V_e \qquad (44)$$

Differentiating the function (44) alone the whole system with the proposed controller (38) and estimators (16), we have :

$$\dot{V} = \dot{H}_d + \dot{V}_e \qquad (45)$$

In Proposition 2, we have shown that the condition $\dot{V}_e \leq 0$ is satisfied under the following condition:

$$0 \leq V_e \leq \frac{c}{K_0} + (V(0) - \frac{c}{K_0})e^{-K_0 t} \qquad (46)$$

We recall that $c = \frac{\xi^2}{4\epsilon}$, where ϵ is a small positive constant, ξ represents the upper bound of $\|\dot{\tau}_d\|$. $K_0 = 2(\lambda_{min}(\alpha) - \epsilon)$, where $\lambda_{min}(\alpha)$ is the smallest eigenvalue of the estimator turning parameter α.

This equation always holds true in condition that the turning parameter α is correctly chosen, as elaborated in detail in Section 4.1.

With regard to the Lyapunov function of the proposed controller, we have recently demonstrated that with appropriately tuning selected parameters S_{11} S_{22} and K_d :

$$\dot{H}_d < 0 \ , \forall z \neq 0_{5\times1} \qquad (47)$$

In conclusion, the validity of $\dot{V} \leq \dot{H}_d + \dot{V}_e$ implies that we can achieve uniformly ultimately bounded (UUB) tracking errors by appropriately tuning selected control parameters S_{11}, S_{22}, K_d, and the estimator parameter α. Therefore, the stability of the desired system can be assured.

□

5. Simulation and experimental validation

In this section, through simulations and experimentation, we present the performances of the closed-loop system with the designed trajectory tracking control for the under-actuated USV. The control objective here is to stabilize the system to follow the trajectory reference defined.

5.1. Numerical simulations under the influence of time-varying disturbances.

The efficacy of the proposed control algorithm is assessed through numerical simulations. In this section, the simulation environment and results are presented.

We choose the initial position at $\begin{bmatrix}x(0), y(0)\end{bmatrix} = \begin{bmatrix}2\text{m}, -4\text{m}\end{bmatrix}$. Furthermore, we select the initial velocity vector $\begin{bmatrix}u(0), v(0), r(0)\end{bmatrix}$ as $\begin{bmatrix}0\text{m/s}, 0\text{m/s}, 0\text{rad/s}\end{bmatrix}$. The disturbance observer's initial state is set to $\tilde{\tau}_d = \begin{bmatrix}0, 0, 0\end{bmatrix}$.

The desired reference trajectory is considered to be a bow shape in the X-Y plane rather than a circular one, which demonstrate the controller's effectiveness by accommodating bidirectional rotations. The trajectory is defined by the equations:

$$\begin{bmatrix} x_d \\ y_d \end{bmatrix} = \begin{bmatrix} 5\sin(0.1\pi t) \\ -5\sin(0.2\pi t) + 5 \end{bmatrix} \tag{48}$$

The external environmental disturbances are produced by the following equation:

$$\tau_d = \begin{bmatrix} 0.01\sin(0.01t) \\ 0.01\cos(0.01t) \\ 0.01\sin(0.02t) \end{bmatrix} \tag{49}$$

Meanwhile, the disturbance represents the USV system due to slowly varying winds, currents, and waves. We consider the estimator gain $\alpha = \text{diag}[500, 500, 500]$. In Figure (4), the error between the estimated disturbances $\tilde{\tau_d}$ and the external environmental disturbances τ_d in x_b,y_b and the rotation direction are shown. It is obviously shown that the designed disturbance observer can quickly track unknown disturbances as the error converges to 0 quickly.

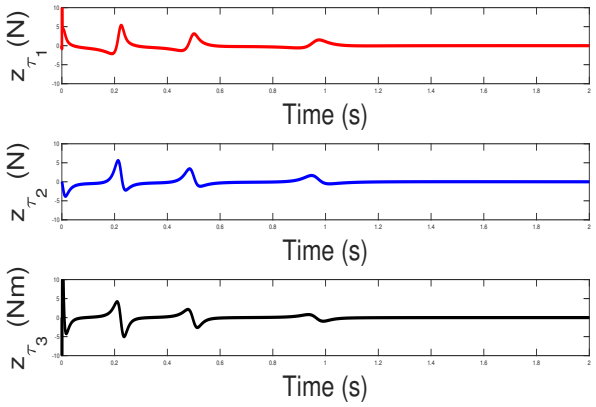

Figure 4: Disturbances estimation (Estimation errors of disturbance in surge direction z_{τ_1}: red solid line, Estimation errors of disturbance in sway direction z_{τ_2} : blue solid line, Estimation errors of disturbance in angular direction z_{τ_3}: black solid line).

We use the control method described in (38) to stabilize the under-actuated USV and track the desired trajectory reference (48) with the disturbance. The design parameters are taken as follows: the damping injection is $S_{22} = [-500, 0, -1700]$, and the controller gain is $K_d = \text{diag}[0.65, 0.65]$.

In the upper part of Figure(5), the red solid line represents the simulation result, while the blue dashed line represents the reference trajectory. Starting from an initial position of $[2\text{m}, -4\text{m}]$, we observe that the USV rapidly converges to the desired reference trajectory. In the lower part of (5), we observe that the errors on X and Y converge asymptotically to zero, which involves the asymptotic convergence of displacement variables to the desired trajectory.

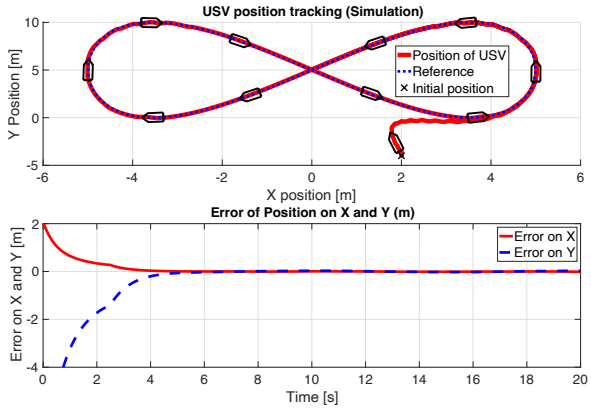

Figure 5: Bow shape trajectory tracking (Upper figure, Reference: blue dashed line, USV position: red solid line) and tracking errors (Lower figure, Error on X: red solid line, Error on Y: blue dashed line).

5.2. *Choice of control parameter*

In this subsection, we discuss the selection criteria for control parameters through a closed-loop simulation aiming to form a circular trajectory in the X-Y plane.

Firstly, we investigate the effect of varying the gain K_d while keeping the damping injection matrix $S_{22} = \text{diag}[-500, 0, -1700]$ fixed. The simulation results are visualized with red and black solid lines, while the reference trajectory is represented by a blue dashed line. Starting from the same initial position. We can notice that in Figure (6) increasing the gain from 2.5 to 0.5 leads to faster convergence of the system, but it may also introduce minor oscillations. This behavior can be analogized to stiffness in a mass-spring system.

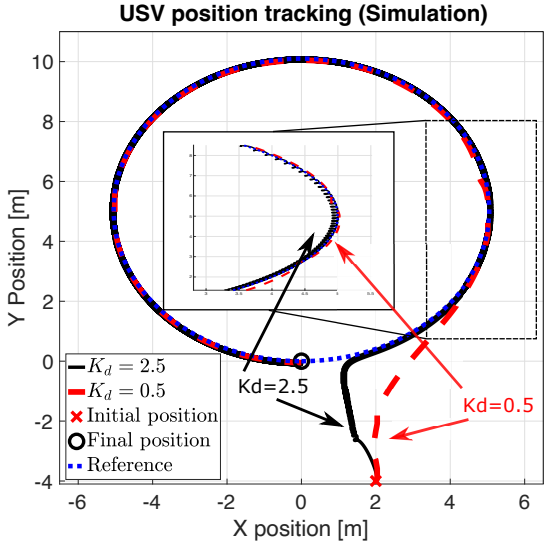

Figure 6: Trajectory tracking with different parameter K_d (Reference: blue dashed line, USV position with $K_d = 2.5$: red dashed line, USV position with $K_d = 0.5$: black solid line).

Secondly, we analyse the impact of the damping injection

matrix S_{22}. While maintaining the controller gain at K_d = diag[0.5, 0.5], S_{22} is then turned from diag[−500, 0, −500] to diag[−1500, 0, −1500]. A reduction in S_{22} results in an increase in oscillations, as shown in Fig 7.

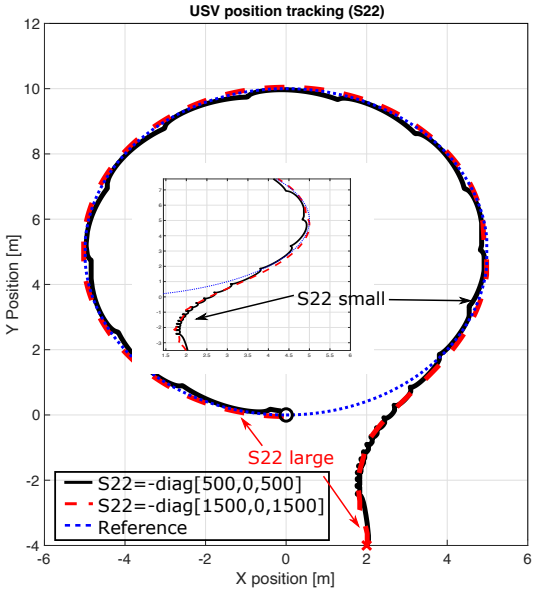

Figure 7: Trajectory tracking with different parameter S_{22}(Reference: blue dashed line, USV position with S_{22} = diag[−1500, 0, −1500] : red dashed line, USV position with S_{22} = diag[−500, 0, −500] : black solid line).

5.3. Experiment validation

Figure 9 illustrates the under-actuated differential-driven USV experimental platform, while the overall system structure is depicted in Figure 8. The USV is outfitted with a 32-bit STM32F407 micro-controller unit (MCU) based on the ARM Cortex-M4 architecture, which is responsible for motion control and sensor data collection. Regarding the control scheme implementation, an on-board computer with an Intel J4125 CPU and 8 GB RAM is employed, running the Robot Operating System (ROS) Neotic for sensor data processing and message communication. The IMU is used to provide the MCU with angular velocity enabling the determination of r and acceleration information. Meanwhile, the GNSS module with the real-time kinematic carrier phase differential technique (RTK) is utilized to obtain the position and, speed information, allowing for the direct determination of x, y. The integration of accelerometer data from the IMU, combined with differential position data from GNSS, is subjected to sensor fusion through Kalman filtering to derive a highly dependable velocity u and v. Subsequently, IMU angular velocity data, in conjunction with angular information derived from RTK, undergoes a comparable Kalman filtering process to achieve a more precise angular estimation ψ. These signals are updated at a frequency of 5 Hz.

Figure 8: The USV experimental platform

The control signal is represented by the PWM duty cycles of the two propeller motors, which can be directly determined from the propulsive forces F_1 and F_2 according to the propeller model in [29]. F_1 and F_2 can be calculated from Equation (9), where F_1 is given by $\frac{\tau_u}{2} + \frac{\tau_r}{B}$ and F_2 is given by $\frac{\tau_u}{2} - \frac{\tau_r}{B}$.

The damping matrix and the Coriolis matrix are derived through hydrodynamic analysis conducted using COMSOL software, see the details in [30]. All the geometric and mass properties pertaining to the USV experimental platform are accessible and presented in Table 1.

Table 1: Geometric and Mass Parameters of the Under-Actuated USV

Width	1 m
Length	1.5 m
Height	0.8 m
Weight	60 kg
Draft (Depth)	0.1 m

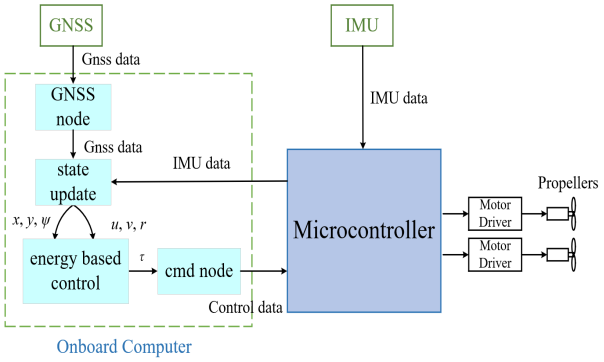

Figure 9: The system structure of experimental platform

In our experimental setup, we consider the desired reference trajectory as a bow shape in the X-Y plane, defined by the equations:

$$\begin{bmatrix} x_d \\ y_d \end{bmatrix} = \begin{bmatrix} 5\sin(0.1\pi t) \\ -5\sin(0.2\pi t) + 5 \end{bmatrix} \tag{50}$$

Initially, we employ estimation techniques (16) to assess the unknown disturbance denoted as τ_d, resulting in the acquisition of $\tilde{\tau}_d$. Subsequently, considering the estimated disturbance, we implement the control law (38), with all parameters provided, measured, and estimated through software.

After experimental tuning, the design parameters are determined as follows: the damping injection values are set as $S_{22} = \text{diag}[-500, 0, -300]$, and the controller gain is defined as $K_d = \text{diag}[0.5, 0.5]$.

In upper part of Figure 10, the X-Y plane depicts a bow shape serving as the reference trajectory. The desired reference trajectory is represented by the blue dashed line while the red solid line denotes the real trajectory.

The lower part of Fig 10 depicts the tracking error in earth frames $x - x_d$ and $y - y_d$, which serve as indicators of the accuracy of the control law. The tracking error is minimal, indicating a high level of precision in the practical control process.

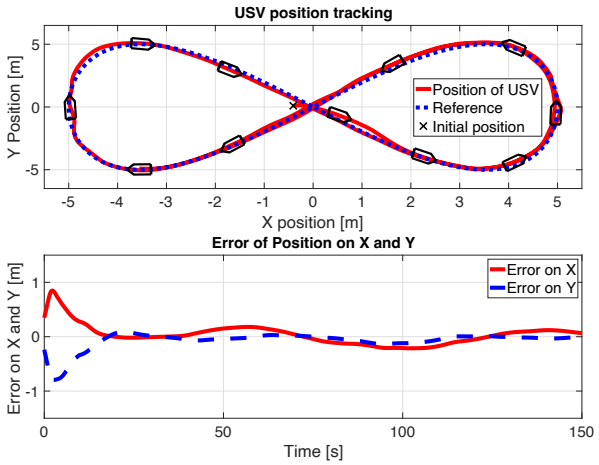

Figure 10: Bow shape trajectory tracking (Upper figure, Reference: blue dashed line, USV position: red solid line) and tracking errors (Lower figure, Error on X: red solid line, Error on Y: blue dashed line).

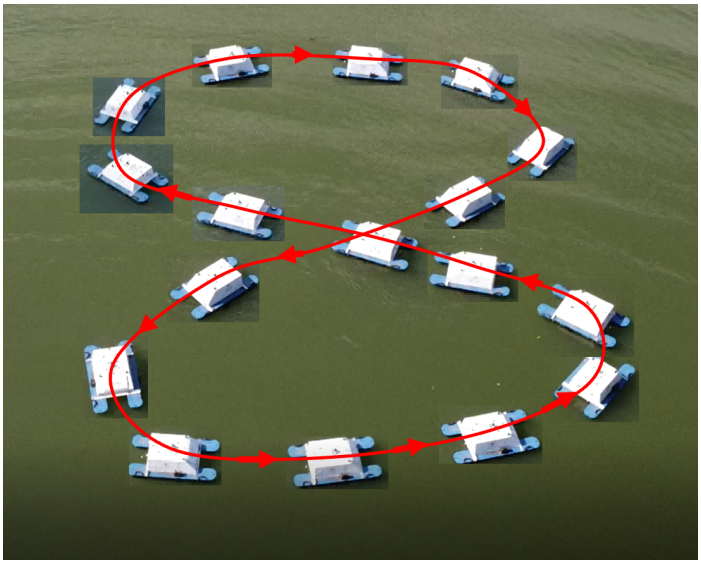

Figure 11: Bow shape trajectory tracking captured by an aerial drone at Qizhen Lake in Zhejiang University.

6. Conclusion

In this paper, we introduced a novel energy-based trajectory tracking control strategy for under-actuated USVs in the presence of unknown environmental disturbances. A passivity-based control model in body-fixed coordinates is developed in the PH framework. An adaptive disturbance estimation method is proposed to accurately estimate the environmental disturbances affecting the motion of USVs. The effectiveness of the proposed controller is demonstrated through simulations and experiments on a USV experimental platform. The results demonstrate the controller's capability to enhance the trajectory tracking performance and effectively counteract the impact of disturbances. The stability of the desired target dynamic system is rigorously proven, highlighting the robustness and reliability of the approach. Overall, the presented control strategy offers a promising solution for enhancing the trajectory tracking capabilities of under-actuated differential-driven USVs in real-world scenarios.

The selection of control parameters relies on the physical nature of the system, such as its stiffness and damping phenomena. Our future work aims to design an adaptive law that can automatically tune the control parameters. This adaptive law will enable the control system to autonomously adjust the parameters based on real-time system feedback. During experimental trials, uncertainties in the model have presented several challenges, although they were addressed by adjusting the control parameters. Moreover, we propose integrating Bayesian optimization into the passivity-based control of under-actuated unmanned surface vessels. By utilizing Bayesian optimization, we can dynamically adjust the model parameters and continuously update and refine the model.

Appendix A. Underactuated USV state variables redefinition

Given three degrees of freedom and only two control variables, control becomes a challenging task. Our objective was to control two degrees of freedom using two control variables. Initially, we considered to omit the dynamics of ψ. However, this would eliminate rotational information in x and y dynamics. Therefore, we involved a fixed reference point δ to incorporate rotation information into x and y dynamics. The logic behind this problem is as follows:

Let us redefine this position $\begin{bmatrix} x_r & y_r \end{bmatrix}^T$ in the earth frame :

$$\begin{aligned} x_r &= x + \delta cos\psi \\ y_r &= y + \delta sin\psi \end{aligned}$$

thus the dynamics of position become :

$$\begin{aligned} \dot{x_r} &= ucos\psi - vsin\psi - r\delta sin\psi \\ \dot{y_r} &= usin\psi - vcos\psi - r\delta cos\psi \end{aligned}$$

We calculate the surge and sway displacements, denoted as s and t, using the above equations, and considering the desired position in the Earth frame :

$$\begin{aligned} s &= (x_r - x_d)cos\psi + (y_r - y_d)sin\psi \\ t &= (y_r - y_d)cos\psi + (x_r - x_d)sin\psi \\ \dot{s} &= rt + u - \dot{x_d}cos\psi - \dot{y}sin\psi \\ \dot{t} &= -rs + v + \delta r + \dot{x_d}sin\psi - \dot{y_d}cos\psi \end{aligned}$$

With this distance between the center of mass and the fixed point, the dynamics of r becomes coupled with the dynamics of x and y then s and t, allows the omission of the dynamics of ψ and reduce the system. This operation aids us in addressing the underactuation issue and formulating an energy-based control method for underactuated systems.

References

[1] T. I. Fossen, M. Breivik, R. Skjetne, Line-of-sight path following of underactuated marine craft, IFAC proceedings volumes 36 (21) (2003) 211–216.

[2] E. Lefeber, K. Y. Pettersen, H. Nijmeijer, Tracking control of an underactuated ship, IEEE transactions on control systems technology 11 (1) (2003) 52–61.

[3] S. He, L. Kou, Y. Li, J. Xiang, Robust orientation-sensitive trajectory tracking of underactuated autonomous underwater vehicles, IEEE Transactions on Industrial Electronics 68 (9) (2020) 8464–8473.

[4] J. Ghommam, F. Mnif, A. Benali, N. Derbel, Asymptotic backstepping stabilization of an underactuated surface vessel, IEEE Transactions on Control Systems Technology 14 (6) (2006) 1150–1157.

[5] Z. Dong, L. Wan, Y. Li, T. Liu, G. Zhang, Trajectory tracking control of underactuated usv based on modified backstepping approach, International Journal of Naval Architecture and Ocean Engineering 7 (5) (2015) 817–832.

[6] Z. Xu, T. Han, W. Zhou, S. He, J. Xiang, Trajectory tracking control for differential-driven unmanned surface vessels considering propeller servo loop, IEEE Transactions on Industrial Informatics (2023) 1–10.

[7] A. P. Aguiar, J. P. Hespanha, Trajectory-tracking and path-following of underactuated autonomous vehicles with parametric modeling uncertainty, IEEE transactions on automatic control 52 (8) (2007) 1362–1379.

[8] D. Chwa, Global tracking control of underactuated ships with input and velocity constraints using dynamic surface control method, IEEE Transactions on control systems technology 19 (6) (2010) 1357–1370.

[9] H. Ashrafiuon, K. R. Muske, L. C. McNinch, R. A. Soltan, Sliding-mode tracking control of surface vessels, IEEE transactions on industrial electronics 55 (11) (2008) 4004–4012.

[10] P. Sarhadi, A. R. Noei, A. Khosravi, Model reference adaptive pid control with anti-windup compensator for an autonomous underwater vehicle, Robotics and Autonomous Systems 83 (2016) 87–93.

[11] A. van der Schaft, B. Maschke, On the hamiltonian formulation of nonholonomic mechanical systems, Reports on mathematical physics 34 (2) (1994) 225–233.

[12] R. Ortega, A. van Der Schaft, B. Maschke, G. Escobar, Interconnection and damping assignment passivity-based control of port-controlled hamiltonian systems, Automatica 38 (4) (2002) 585–596.

[13] R. Ortega, A. J. van Der Schaft, I. Mareels, B. Maschke, Putting energy back in control, IEEE Control Systems Magazine 21 (2) (2001) 18–33.

[14] Y. Yeh, N. Cisneros, Y. Wu, K. Rabenorosoa, Y. Le Gorrec, Modeling and position control of the hasel actuator via port-hamiltonian approach, IEEE Robotics and Automation Letters 7 (3) (2022) 7100–7107.

[15] W. Zhou, Y. Wu, H. Hu, Y. Li, Y. Wang, Port-hamiltonian modeling and ida-pbc control of an ipmc-actuated flexible beam 10 (9) (2021) 236.

[16] A. Mattioni, Y. Wu, H. Ramirez, Y. Le Gorrec, A. Macchelli, Modelling and control of an ipmc actuated flexible structure: A lumped port hamiltonian approach, Control Engineering Practice 101 (2020) 104498.

[17] N. Liu, Y. Wu, Y. Le Gorrec, Energy-based modeling of ionic polymer–metal composite actuators dedicated to the control of flexible structures, IEEE/ASME Transactions on Mechatronics 26 (6) (2021) 3139–3150.

[18] E. P. Ayala, Y. Wu, K. Rabenorosoa, Y. Le Gorrec, Energy-based modeling and control of a piezotube actuated optical fiber, IEEE/ASME Transactions on Mechatronics 28 (1) (2022) 385–395.

[19] J. G. Romero, A. Donaire, R. Ortega, Robust energy shaping control of mechanical systems, Systems & Control Letters 62 (9) (2013) 770–780.

[20] T. Perez, A. Donaire, C. Renton, F. Valentinis, Energy-based motion control of marine vehicles using interconnection and damping assignment passivity-based control–a survey, IFAC Proceedings Volumes 46 (33) (2013) 316–327.

[21] C. Lv, H. Yu, J. Chi, T. Xu, H. Zang, H. lue Jiang, Z. Zhang, A hybrid coordination controller for speed and heading control of underactuated unmanned surface vehicles system, Ocean Engineering 176 (2019) 222–230.

[22] C. Lv, H. Yu, N. Zhao, J. Chi, H. Liu, L. Li, Robust state-error port-controlled hamiltonian trajectory tracking control for unmanned surface vehicle with disturbance uncertainties, Asian Journal of Control 24 (1) (2022) 320–332.

[23] A. Donaire, J. G. Romero, T. Perez, Trajectory tracking passivity-based control for marine vehicles subject to disturbances, Journal of the Franklin Institute 354 (5) (2017) 2167–2182.

[24] R. Reyes-Báez, A. van der Schaft, B. Jayawardhana, A. Donaire, T. Pérez, Tracking control of marine craft in the port-hamiltonian framework: A virtual differential passivity approach, in: 2019 18th European Control Conference (ECC), IEEE, 2019, pp. 1636–1641.

[25] A. van der Schaft, L2-gain and passivity techniques in nonlinear control, Springer, 2000.

[26] T. I. Fossen, Marine control systems–guidance. navigation, and control of ships, rigs and underwater vehicles, Marine Cybernetics, Trondheim, Norway, Org. Number NO 985 195 005 MVA, www. marinecybernetics. com, ISBN: 82 92356 00 2 (2002).

[27] T. I. Fossen, Guidance and control of ocean vehicles, University of Trondheim, Norway, Printed by John Wiley & Sons, Chichester, England, ISBN: 0 471 94113 1, Doctors Thesis (1999).

[28] A. Astolfi, R. Ortega, Immersion and invariance: A new tool for stabilization and adaptive control of nonlinear systems, IEEE Transactions on Automatic control 48 (4) (2003) 590–606.

[29] T. I. Fossen, M. Blanke, Nonlinear output feedback control of underwater vehicle propellers using feedback form estimated axial flow velocity, IEEE Journal of oceanic Engineering 25 (2) (2000) 241–255.

[30] S. He, L. Kou, Y. Li, J. Xiang, Position tracking control of fully-actuated underwater vehicles with constrained attitude and velocities, IEEE Transactions on Industrial Electronics 69 (12) (2022) 13192–13202.